Phonon Modes at the 2H-$NbSe_2$ Surface Observed by Grazing Incidence Inelastic X-Ray Scattering

B. M. Murphy,[1,2] H. Requardt,[3] J. Stettner,[1] J. Serrano,[3] M. Krisch,[3] M. Müller,[1] and W. Press[1,4]

[1]*Institut für Experimentelle und Angewandte Physik, Christian-Albrechts-Universität, D-24098 Kiel, Germany*

[2]*CCLRC Daresbury Laboratory, Warrington, Cheshire WA4 4AD, United Kingdom*

[3]*ESRF, BP 220, F-38043 Grenoble Cedex 9, France*

[4]*Institut Laue-Langevin, BP 156, F-38042 Grenoble Cedex 9, France*

(Received 20 January 2005; revised manuscript received 9 August 2005; published 16 December 2005)

We have determined the dispersion of acoustic and optical surface phonon modes at the 2H-$NbSe_2$ by inelastic x-ray scattering under grazing incidence conditions. Already, at room temperature, an anomaly is observed close to the charge density wave Q-vector position located at about one-third along the Γ-M direction of the Brillouin zone. Our results indicate that the anomaly for the surface mode occurs at a lower energy than that measured in bulk sensitive geometry in the same experiment, showing evidence of a modified behavior in the uppermost layers. We demonstrate that inelastic x-ray scattering in grazing incidence conditions provides a unique tool to selectively study either surface or bulk lattice dynamics in a single experiment.

DOI: 10.1103/PhysRevLett.95.256104 PACS numbers: 68.49.−h, 63.22.+m, 68.35.Ja, 71.45.Lr

The layered transition metal dichalcogenides exhibit fascinating properties due to their van der Waals bonded layered structure: superconducting behavior, nonlinear and anisotropic electrical properties, very large dielectric constants, charge density wave (CDW) instabilities and a wealth of dynamical features [1]. $NbSe_2$ is a member of this group of materials. As a result of its layerlike structure, $NbSe_2$ displays almost two-dimensional behavior [2–4]. For the 2H polytype, the structure arises from the stacking of hexagonally packed planes ($a = 3.443$ Å, $c = 12.547$ Å [5]) with van der Waals and Coulomb forces between the layers. A structural phase transition accompanied by a CDW distortion occurs at approximately 33 K [2–4]. This CDW is incommensurate with a wave vector $Q \sim (a^*/3, 0, 0)$, where $a^* = 4\pi/\sqrt{3}a$, and is reported not to lock-in over the temperature range from 32 to 5 K [2,3]. The intensity of the hexagonal superlattice reflection was shown to decrease *monotonically* to zero, a behavior consistent with a second-order transition. Though the origin of these instabilities is not fully understood, angle-resolved photoemission experiments suggest that Fermi nesting plays an important role in the CDW formation [6–8]. Inelastic neutron scattering (INS) studies revealed a Kohn-like anomaly [2] for the two lowest longitudinal Σ_1 phonon branches. The ω_1 branch displays softening over the 100–33 K temperature range at $Q = (a^*/3, 0, 0)$ [4]. Evidence for differences between bulk and surface properties of 2H-$NbSe_2$ come from grazing incidence x-ray diffraction experiments [9,10] and a surface phonon study using helium scattering [11]. The diffraction study revealed that the $(a^*/3, 0, 0)$ satellite reflection intensity monotonically decreases across the CDW transition both in the bulk and at the surface, but a higher transition temperature was observed at the surface. The He scattering work reports a weak anomaly in the surface phonon dispersion curves, but in contrast to the bulk INS measurements, it occurs at 3/5 of the Brillouin zone boundary. As He scattering is a purely surface sensitive technique accessing only the surface layer, a direct comparison with the bulk behavior was not possible.

The aim of the present Letter is to shed light on the difference between surface and bulk dynamics, in particular, to clarify the influence of the surface and the weak interlayer coupling on the CDW related phonon modes. To this purpose we conducted an inelastic x-ray scattering (IXS) experiment in grazing incidence geometry on a single crystal of 2H-$NbSe_2$. By tuning the angle of incidence either below or above the critical angle of total reflection, the surface and bulk dynamics are selectively probed, thus allowing direct comparison in a single experiment.

The experiment was carried out on beam line ID28 at the European Synchrotron Radiation Facility (ESRF). The instrument was operated at an incident photon energy of 17.794 keV, using the Si (9 9 9) reflection order for the high-energy resolution monochromator and analyzer crystals, and providing an instrumental energy resolution of 3 meV, i.e., elastic line full width half maximum (FWHM). The available incident beam dimensions of 250×60 μm (horizontal × vertical; FWHM) were reduced in the vertical plane to 12 μm in order to limit the beam footprint to the length of the sample. A platinum-coated mirror was inserted before the sample in order to deflect the primary beam downwards onto the sample surface. Using this deflector in combination with the sample tilt angles, incidence and exit angles (α_i and α_f) around the critical angle of total external reflection, $\alpha_c = 0.154°$ for 2H-$NbSe_2$, could be obtained. The sample used in the present study had dimensions of $8 \times 4 \times 1$ mm^3, and was prepared by iodine vapor transport, using a narrow ampoule with a long

two-stage annealing process, at Bell Laboratories [12]. This process resulted in a high-quality, thick crystal with a low mosaic width [$0.0045 \pm 0.0001°$ FWHM for the (002) reflection], appropriate for grazing incidence diffraction. The sample was cleaved prior to measurements using adhesive tape, and mounted with its (00l) surface horizontal in a vacuum chamber. α_i and α_f were set to $\alpha_c 0.03°$. In this configuration the angle of incidence remained below the critical angle, but the experiment benefited from the enhancement in the transmission function close to α_c [13]. The x-ray penetration depth, defined as the decay to $1/e$ of the incident electromagnetic field, is about 4 nm [13]. The topmost 2.7 nm contributed 50% to the scattered signal due to the exponential decay. These surface sensitive data were complemented by bulk measurements, accomplished with the same experimental setup by increasing α_i and α_f to $\alpha_c + 0.03°$, and therefore penetrating further into the sample, achieving a scattering depth of $\sim$100 nm. Constant-Q scans were recorded for the longitudinal acoustic and optical branches along the $(\xi, 0, 0)$ direction (from 0.05 to 0.45) around the (200) surface reflection. The data were collected with the standard analyzer opening of 20×60 mm^2 (horizontal $\times$ vertical) 6.5 m beyond the sample position, providing a Q resolution of about $\Delta Q = 0.216$ nm^{-1} in the scattering plane [14]. Each scan at a given Q position took about three and a half hours, and in some cases two scans were summed up.

Typical energy scans of the acoustic and optic phonons at room temperature containing both Stokes and anti-Stokes contributions are shown in Fig. 1 for surface and bulk sensitive measurements. An elastic component and a number of inelastic peaks are observed. The background

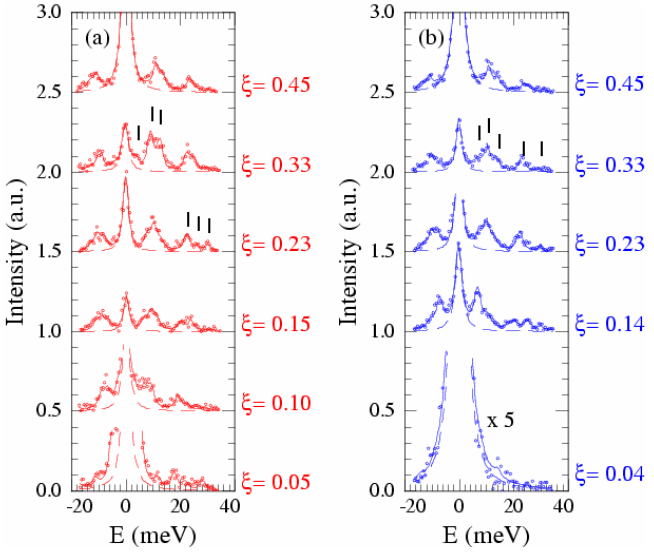

FIG. 1 (color online). Grazing incidence IXS spectra of 2H-$NbSe_2$ (a) surface ($\alpha_i = \alpha_c - 0.03°$) and (b) bulk ($\alpha_i = \alpha_c + 0.03°$) along the $[\xi, 0, 0]$ direction at room temperature. (Raw data: open circles. Solid line: best fit results. Dashed curve: elastic component/energy resolution.)

was less than 1×10^{-3} counts/s. At small ξ, i.e., close to the (200) reflection, it is difficult to separate the acoustic phonon peak from the lowest optical mode, as the instrument resolution is similar to the mode energy. The energy position and intensity of the inelastic features have been fitted using a standard χ^2 minimization [15], utilizing a damped harmonic oscillator profile convoluted with the energy resolution profile (modeled by a Lorentz profile). The FWHM of the elastic peak from the $NbSe_2$ sample was determined to be 2.6 ± 0.2 meV. This value was used in fitting all spectra. Five peaks were included in the fit; one acoustic phonon mode and four optic phonon contributions as previously assigned [2,16]. The predominantly longitudinal Σ_1 modes are intense. In addition, small contributions from some of the Σ_3 branches, predominantly of transverse nature, are also visible. While in both configurations the ω_2 mode has a similar value at $\xi = 0.23$, the IXS spectra at $\xi = 0.33$ display one significant difference. This is emphasized in Fig. 2, where the surface sensitive IXS spectrum is shown in Fig. 2(a), and the comparison between surface and bulk sensitive measurement is displayed in Fig. 2(b). There is clearly an inelastic component present at lower energy in the surface data than in the bulk data (see Fig. 2). The ω_2 mode softens to 6.8 meV at $\xi = 0.33$ in the bulk and an even greater softening is observed at the surface (4 meV). The ω_1 mode has an energy of $\sim$5 meV at $\xi = 0.05$, also displaying softening for both surface and bulk sensitive geometry at $\xi = 0.33$ though less pronounced than that of the acoustic branch.

Figure 3 provides an overview of the determined phonon dispersions and a comparison with previous INS results as well as calculations. We succeeded in resolving the Σ_1 modes ω_1 and ω_2 along the Γ-M direction of the Brillouin zone as reported only at $Q = (a^*/3, 0, 0)$ by Ayache *et al.* [4] and two additional optical bands at higher energy previously observed at $Q = 0$ in Raman experiments [17]. Our data span a Q range from $\xi = 0.05$ to 0.45, thus providing an extended insight into 2H-$NbSe_2$ lattice dynamics. The overall form of the experimental dispersion relation, with the exception of the surface anomaly, (see Fig. 3) agrees well with the bulk calculations from Feldman [18] (solid lines) and Motizuki *et al.* [16] (dashed lines), which included an effective ion-ion interaction. Both for the surface and bulk case, Σ_1 modes, ω_1 and ω_2 are observed below 10 meV at low Q. The acoustic ω_2 mode shows a dip in its increase at $\xi = 0.33$ at the CDW satellite position, followed by an energy increase for even larger ξ. The approximate value of the sound velocity has been determined from the slope of the ω_2 mode to be $(57 \pm 10) \times 10^4$ cm/s in the bulk sensitive measurements and $(50 \pm 20) \times 10^4$ cm/s in the surface sensitive geometry. Benedek *et al.* carried out helium atom scattering experiments on 2H-$NbSe_2$, where they observed a surface phonon anomaly with a slight Q shift from $\xi = 0.33$ to 0.3 [11]. In the present experiment, a general softening is

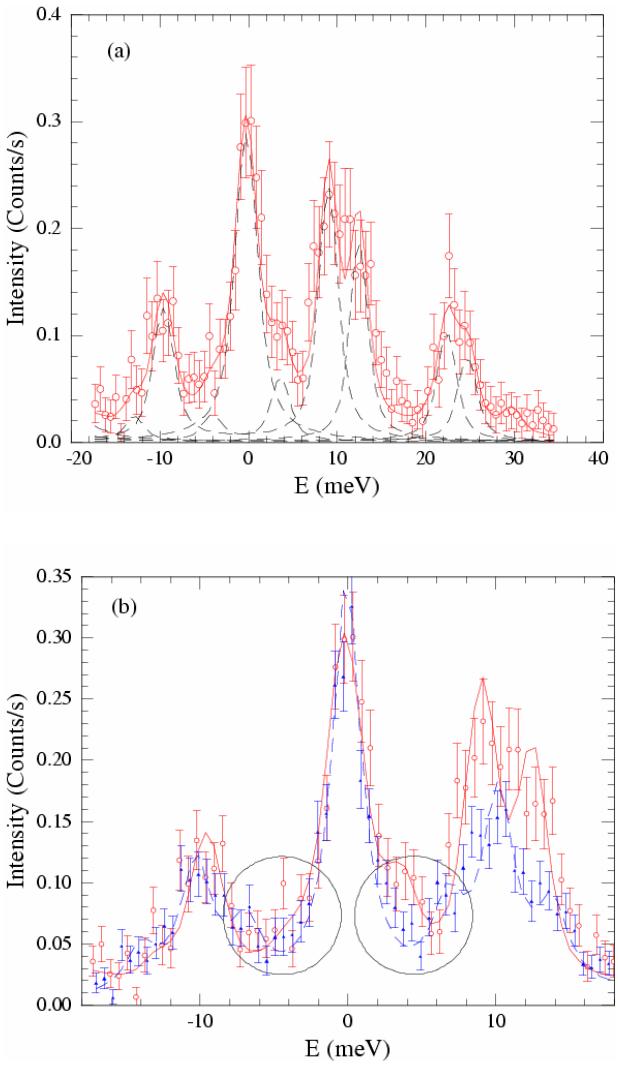

FIG. 2 (color online). (a) Surface grazing incidence IXS spectrum of $2H$-$NbSe_2$ at $T = 300$ K, taken at $\xi = 0.33$. Experimental data (○) are shown with error bars and the best fit (solid line). (b) Comparison of surface (solid line) and bulk (dashed line) data collected at $\xi = 0.33$ overlaid.

observed at ξ near to 0.33, thus points at a strong interaction between the phonons and the conduction electrons. The dip at 0.33 is greater at the surface than in the bulk. Our results are consistent with those of Moncton *et al.* [2] for bulk $2H$-$NbSe_2$ and, in particular, with energy integrated x-ray grazing-incidence diffraction measurements where no change of position of the surface CDW peak is observed with respect to the bulk [9]. The phonon anomaly is observed close to the CDW satellite position in the Σ_1 ω_2 mode indicating that this branch also plays an important role in CDW transition.

In summary, we have measured the bulk and surface phonon dispersion relations for $2H$-$NbSe_2$ at 300 K, by selectively measuring in surface- and bulk- sensitive geometry by means of grazing incidence inelastic x-ray scattering varying depth sensitivity from 4 to 100 nm.

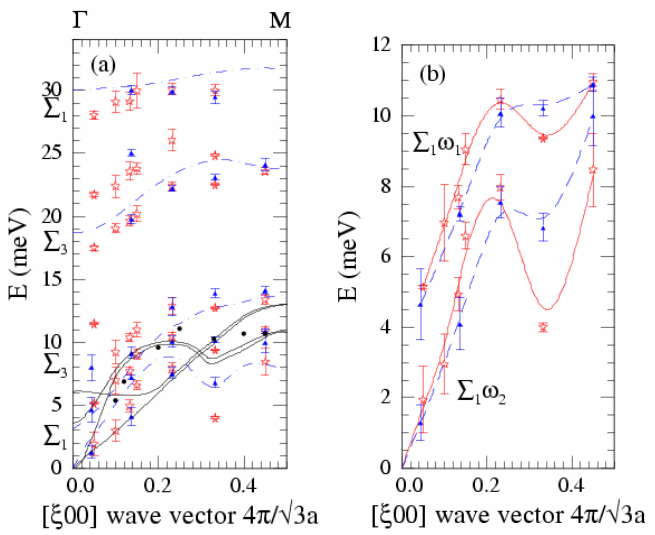

FIG. 3 (color online). (a) Room temperature surface (open stars) and bulk (filled triangles) phonon dispersion curve of $2H$-$NbSe_2$, as obtained by means of grazing incidence IXS. $\xi = 2 - h$ in reciprocal space units. The Σ_1 ω_1, ω_2 modes and the Σ_3 acoustic and optic modes in the bulk and in the surface are shown, as well as two additional optical modes (Σ_1, Σ_3). Bulk sensitive INS data (solid circles) from [2] are shown for comparison. Solid and dashed lines display the curves calculated in [16,18] respectively. (b) Enlarged view of the low energy part of the phonon dispersion (lines are a guide to the eye).

This is the first time such a comprehensive data set, comprising the longitudinal acoustic and three optical branches throughout the whole Brillouin zone, has been collected for a transition metal dichalcogenide layered crystal in a single experiment. For both bulk and surface data at room temperature an anomaly is observed at $\xi = 0.33$. This anomaly is far more pronounced in the surface sensitive data. The position agrees with theoretical predictions and is similar to that observed previously in the bulk. This result gives evidence that some change is occurring in the topmost layers. One possibility is that the surface electronic state cuts the Fermi surface at a different position than the bulk Fermi wave vector, as predicted by Benedek *et al.* [11]. Another possibility would involve an increased electron-phonon interaction, which is consistent with the change of symmetry and coordination of the upper atomic layers with respect to that of the bulk. More generally, this experiment shows that IXS under grazing incidence conditions provides a powerful spectroscopic tool to study surface and bulk lattice dynamics in a single experiment providing the possibility to tune depth sensitivity between 2 to 1000 nm, thus complementing helium scattering [11], high-resolution electron-energy loss experiments [19] and bulk studies by INS experiments.

We are indebted to Peter Hatton for providing the $NbSe_2$ crystal. We acknowledge the European Synchrotron Radiation Facility for provision of beam time and we would like to thank Denis Gambetti and Keith Martel for

the technical assistance in the development of the grazing incidence setup. This work was supported by the German DFG Grant No. FOR 353/2-2. B. M. Murphy would like to thank Lutz Kipp, Felix Tuczek, and Metin Tolan for productive discussion and support.

[1] J. A. Wilson, F. J. DiSalvo, and S. Mahajan, Phys. Rev. Lett. **32**, 882 (1974).
[2] D. E. Moncton, J. D. Axe, and F. J. DiSalvo, Phys. Rev. Lett. **34**, 734 (1975); D. E. Moncton, J. D. Axe, and F. J. DiSalvo, Phys. Rev. B **16**, 801 (1977).
[3] C.-H. Du *et al.*, J. Phys. Condens. Matter **12**, 5361 (2000).
[4] C. Ayache, R. Currat, and P. Molinié, Physica B (Amsterdam) **180**, 333 (1992).
[5] A. Meerschaut and C. Deudon, Mater. Res. Bull. **36**, 1721 (2001).
[6] Th. Straub *et al.*, Phys. Rev. Lett. **82**, 4504 (1999).
[7] Y. Yokoya *et al.*, Science **294**, 2518 (2001).
[8] K. Rossnagel *et al.*, Phys. Rev. B **64**, 235119 (2001).
[9] B. M. Murphy *et al.*, Physica B (Amsterdam) **336**, 103 (2003).
[10] B. M. Murphy, J. Stettner, M. Muller, and W. Press (to be published).
[11] G. Benedek, L. Miglio, and G. Seriani, in *Helium Atom Scattering From Surfaces*, edited by E. Hulpke, Springer Series in Surface Science (Springer-Verlag, New York, 1992), Vol. 27, 208.
[12] C. S. Oglesby, E. Bucher, C. Kloc, and H. Hohl, J. Cryst. Growth **137**, 289 (1994).
[13] H. Dosch, Phys. Rev. B **35**, 2137 (1987).
[14] H. Requardt, J. E. Lorenzo, P. Monceau, R. Currat, and M. Krisch, Phys. Rev. B **66**, 214303 (2002).
[15] MINUIT, D516-CERN, Computer 7600, Interim Program Library.
[16] K. Motizuki, K. Kimura, E. Ando, and N. Suzuki, J. Phys. Soc. Jpn. **53**, 1078 (1984).
[17] L. Miglio and L. Colombo, Phys. Rev. B **37**, 3025 (1988).
[18] J. L. Feldman, Phys. Rev. B **25**, 7132 (1982).
[19] J. Hiller and R. F. Baker, J. Appl. Phys. **15**, 663 (1944).